AIP | Applied Physics Letters

Influence of the material parameters on quantum cascade devices

E. Benveniste, A. Vasanelli, A. Delteil, J. Devenson, R. Teissier, A. Baranov, A. M. Andrews, G. Strasser, I. Sagnes, and C. Sirtori

Citation: Applied Physics Letters **93**, 131108 (2008); doi: 10.1063/1.2991447
View online: http://dx.doi.org/10.1063/1.2991447
View Table of Contents: http://scitation.aip.org/content/aip/journal/apl/93/13?ver=pdfcov
Published by the AIP Publishing

Articles you may be interested in

Spectroscopic method of strain analysis in semiconductor quantum-well devices
J. Appl. Phys. **96**, 4056 (2004); 10.1063/1.1791754

Strain effects, electronic parameters, and electronic structures in modulation-doped In x Ga 1−x As/In y Al 1−y As coupled step-rectangular quantum wells
J. Appl. Phys. **94**, 7621 (2003); 10.1063/1.1631078

Band parameters for nitrogen-containing semiconductors
J. Appl. Phys. **94**, 3675 (2003); 10.1063/1.1600519

Nonresonant nonlinearity due to intersubband transitions in nonparabolic semiconductor quantum wells
J. Appl. Phys. **90**, 5441 (2001); 10.1063/1.1412264

Band structure nonlocal pseudopotential calculation of the III-nitride wurtzite phase materials system. Part I. Binary compounds GaN, AlN, and InN
J. Appl. Phys. **88**, 6467 (2000); 10.1063/1.1309046

Confidently measure down to 0.01 fA and up to 10 PΩ
Keysight B2980A Series Picoammeters/Electrometers
View video demo>
KEYSIGHT TECHNOLOGIES

This article is copyrighted as indicated in the article. Reuse of AIP content is subject to the terms at: http://scitation.aip.org/termsconditions. Downloaded to IP: 131.230.73.202 On: Thu, 18 Dec 2014 18:35:51

Influence of the material parameters on quantum cascade devices

E. Benveniste,[1] A. Vasanelli,[1,a)] A. Delteil,[1] J. Devenson,[2] R. Teissier,[2] A. Baranov,[2] A. M. Andrews,[3] G. Strasser,[3] I. Sagnes,[4] and C. Sirtori[1]
[1]*Laboratoire "Matériaux et Phénomènes Quantiques," Université Paris Diderot, CNRS-UMR 7162, F-75013 Paris, France*
[2]*Institut d'Electronique du Sud, Université Montpellier 2, CNRS-UMR 5214, F-34095 Montpellier, France*
[3]*Center for Micro- and Nanostructures, TU Vienna, A-1040 Vienna, Austria*
[4]*Laboratoire de Photonique et de Nanostructures, CNRS-UPR20, Route de Nozay, F-91460 Marcoussis, France*

(Received 1 August 2008; accepted 9 September 2008; published online 2 October 2008)

An experimental investigation on the influence of the material systems on the optical properties of quantum cascade structures is presented. Three electroluminescent quantum cascade devices have been grown using GaAs/AlGaAs, GaInAs/AlInAs, and InAs/AlSb heterostructures. The devices emit at 10 μm and are based on a similar bandstructure design. Our results verify that the optical quantum efficiency has the predicted dependence on the electron effective mass. We also demonstrate that the shape of the electroluminescence spectra is independent from the particular material parameters and mainly depends on the tunnel coupling between the injector state and the upper state of the radiative transition. © *2008 American Institute of Physics*.
[DOI: 10.1063/1.2991447]

The quantum cascade laser (QCL) is a semiconductor laser based on intersubband transitions in quantum wells, first demonstrated in 1994 (Ref. 1) by using a GaInAs/AlInAs active region. In this device the principles of operation are independent of the specific semiconductor system, as they arise from the sequence of potential wells forming the heterostructure. Nevertheless, it took about four years before a QCL could be realized in the GaAs/AlGaAs (Ref. 2) material system and nine years to demonstrate it in a less conventional structure such as InAs/AlSb.[3,4] On one hand this lag is related to material growth and development and on the other hand to the fundamental differences between the material systems, which introduce substantial changes in the design of the active regions and the waveguides.

The aim of our investigation is to determine the weight of the material parameters (such as effective mass, phonons, alloy disorder, and interface roughness) on the gain in the different material systems. The gain for a given emission wavelength is proportional, if neglecting the lower state population, to the product $\eta=|z_{21}|^2\times\tau_2$, where z_{21} is the dipole matrix element between the upper and lower states of the laser transition and τ_2 is the upper state lifetime. By considering the dependence of τ_2 and z_{21} on the electron effective mass m_e^*, it is possible to show that η is proportional to $(m_e^*)^{-3/2}$. It is quite difficult to extract this dependence when directly comparing QCL performance due to the differences in the active region designs, optical confinement, and waveguide losses. In order to eliminate all of these dissimilarities, we compare the optical characteristics of three quantum cascade electroluminescent devices, emitting at 10 μm and based, respectively, on GaInAs/AlInAs, GaAs/$Al_{0.45}Ga_{0.55}As$, and InAs/AlSb material systems.[5] For simplicity, the active region consists of a single quantum well, where the radiative transition takes place, and an injection/extraction miniband. Figure 1 presents a simplified scheme of the conduction band diagram under an applied electric field. Electrons are injected into the excited subband of the quantum well (state labeled 2) through an injector state *R*. After relaxation from subband 2 to subband 1 by either radiative or nonradiative (LO-phonon emission, interface roughness scattering, and alloy disorder) transitions, electrons are extracted through the miniband and injected into the following period. The well width is chosen in order to have the same emission wavelength, 10 μm, in the three material systems (see Table I). These structures are not designed to show population inversion. The interesting quantity for their comparison is the quantum efficiency QE, defined as the ratio between the luminescence signal and the injected current. The quantum efficiency is also proportional to η and we will verify its dependence on the effective mass.

For electrical and optical characterizations, samples were processed into mesas. For InAs/AlSb samples we realized square mesas (80×80 μm^2) with nonalloyed Cr–Au contacts; for GaAs and GaInAs samples we realized circular mesas (200 μm diameter) with alloyed Ni–Au–Ge contacts. The substrate was polished at an angle of 45° with respect to

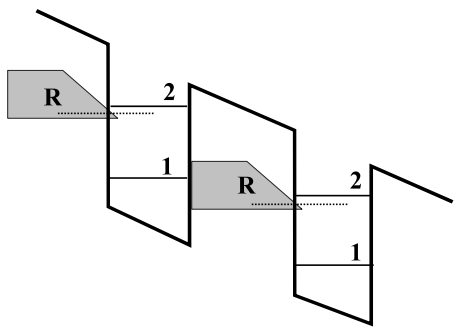

FIG. 1. Schematic energy band diagram of two periods of a QC device. The radiative transition involves the levels labeled 2 and 1 in the main quantum well. The injector state is labeled *R*.

a)Electronic mail: angela.vasanelli@univ-paris-diderot.fr.

 © 2008 American Institute of Physics

This article is copyrighted as indicated in the article. Reuse of AIP content is subject to the terms at: http://scitation.aip.org/termsconditions. Downloaded to IP: 131.230.73.202 On: Thu, 18 Dec 2014 18:35:51

TABLE I. Summary of the quantities used for the comparison of the three devices. The inelastic lifetime is obtained by considering the electron-LO-phonon interaction. The elastic lifetime includes interface roughness scattering for the three material systems and alloy disorder for the GaInAs structure.

	InAs	GaInAs	GaAs
Quantum well width (Å)	148	102	86
No. of periods	10	20	20
τ_{LO} (ps)	1.57	1.04	0.94
$\tau_{elastic}$ (ps)	6.78	3.1	4.9
Dipole matrix element (Å)	30.2	22.9	18.2
Emission energy (meV)	128	130	120

the growth axis to collect the luminescence. Measurements were performed in pulsed operation at 77 K.

Figure 2 shows the light-current characteristics per period (symbols) and their linear fit (lines). We can see that the QE is constant. The ratio between the slopes measured for the three devices is consistent with the ratio of the different m_e^* (see Table II). The experimental conditions for the *L-I* measurements were kept identical for the three devices in order to neglect corrections coming from the collection efficiency.

We model our system by observing that the electroluminescence signal contains two components: radiative transitions from subband 2 to subband 1 ("direct transition") and from R to 1 ("diagonal transition") (see Fig. 3). The density of photons emitted per period and per unit time is thus proportional to $(n_2/\tau_{21}^{rad}+n_R/\tau_{R1}^{rad})$, where τ_{21}^{rad} (τ_{R1}^{rad}) is the spontaneous emission lifetime for the $2\rightarrow1$ $(R\rightarrow1)$ transition and n_2 (n_R) is the population of subband 2 (R). By solving a system of rate equations, with the approximation $E_{21}\approx E_{R1}$, we find $\mathrm{QE}\propto((1/\tau_2)+(1/\tau_R))^{-1}(z_{21}^2+z_{R1}^2)$, where τ_2 (τ_R) is the nonradiative lifetime for subband 2 (R) and z_{21} (z_{R1}) is the dipole matrix element for the $2\rightarrow1$ $(R\rightarrow1)$ transition. The total oscillator strength[6] of the system is concentrated between $2\rightarrow1$ and $R\rightarrow1$ transitions; thus the sum of the squares of the dipole matrix elements is constant with the current. Analogously, the total lifetime $((1/\tau_2)+(1/\tau_R))^{-1}$ of the anticrossed states 2 and R does not vary with the applied bias. As a consequence, the QE is constant with the current during injection and is proportional to η. We evaluate the theoretical ratio between the quantum efficiencies of the three devices by calculating η in a three band $\mathbf{k}\cdot\mathbf{p}$ model.[6] We also take into account the differences in the emission energy of the three devices (see Table I) by multiplying η by the correction term E_{21}[4,7]. The parameters used for the calculation of the energy dependent effective mass, as well as the

TABLE II. Comparison of the experimental and the calculated ratios between the QEs for the couple of material systems of the first column.

QE ratio	Expt.	$\mathbf{k}\cdot\mathbf{p}$ model	$(m_e^*)^{-3/2}$
InAs / GaInAs	2.4	2.7	2.7
GaInAs / GaAs	2.1	2.2	1.8
InAs / GaAs	5.2	5.7	5.0

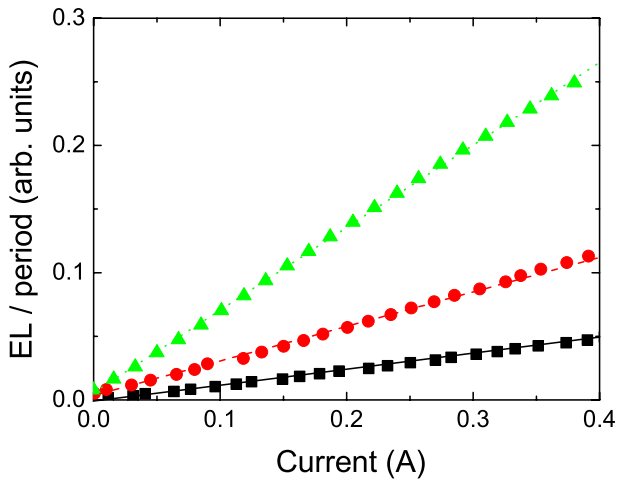

FIG. 2. (Color online) Light-current characteristics in pulsed operation (500 ns at 100 kHz) at 77 K for InAs/AlSb (triangles), GaInAs/AlInAs (circles), and GaAs/AlGaAs (squares). The lines are the result of a linear fit of the experimental data.

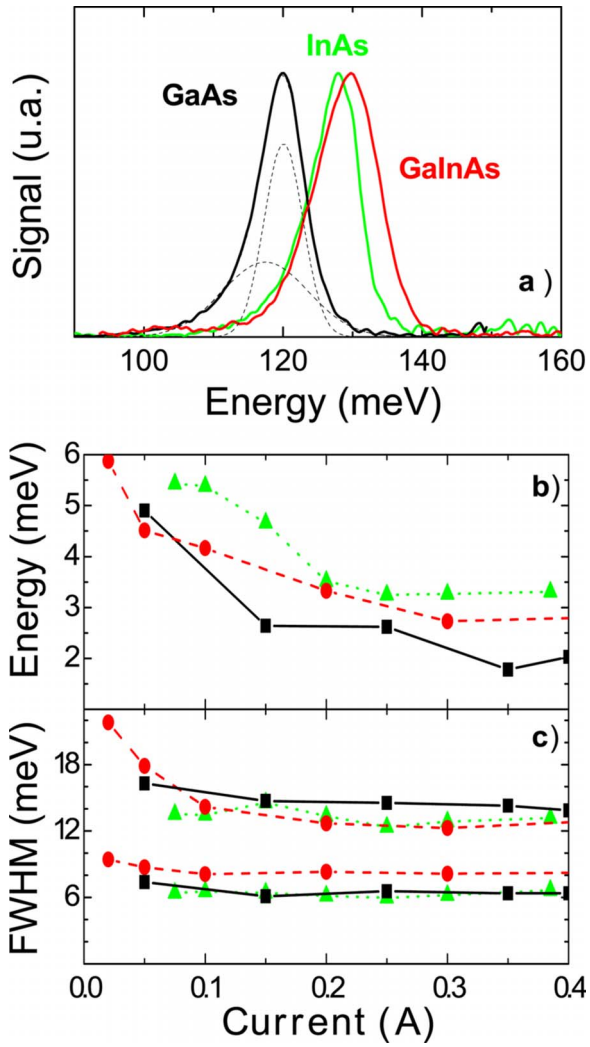

FIG. 3. (Color online) (a) Electroluminescence spectra measured at 77 K and 5% duty cycle for GaInAs (at 200 mA), InAs (at 250 mA), and GaAs (at 250 mA). The dashed lines indicate the two Gaussian functions and the result of the fit for the GaAs spectrum. (b) ΔE as a function of the injected current for InAs (triangles), GaAs (squares), and GaInAs (circles). (c) FWHM of the two Gaussian functions resulting from the fit of the experimental spectra. The larger peak is related to the diagonal transition.

This article is copyrighted as indicated in the article. Reuse of AIP content is subject to the terms at: http://scitation.aip.org/termsconditions. Downloaded to IP: 131.230.73.202 On: Thu, 18 Dec 2014 18:35:51

LO-phonon energy, the interface roughness, and the alloy disorder parameters have been determined in previous work[8–10] by means of electron scattering spectroscopy by high magnetic field. The values of the nonradiative lifetimes, as well as of the dipole matrix elements, are reported in Table I. The elastic lifetime of GaInAs is shorter than those of the other material systems due to alloy disorder. The second and third columns of Table II present, respectively, the ratio between the QE obtained from the fit of the *L-I* curves and from the calculation for the couples of material systems of the first column. The agreement is very good. The last column presents the ratio between the $(m_e^*)^{-3/2}$. Hence, the QE has the expected dependence on the electron effective mass.

Figure 3(a) shows the electroluminescence spectra. They are centered at approximately the same energy (see Table I). Moreover, the three spectra present the same shape. In the entire current range where the $L-I$ characteristics are linear, the spectra can be extremely well fitted by the sum of two Gaussian functions, as shown in Fig. 3(a) for the GaAs device. The low energy Gaussian function blueshifts when increasing the voltage applied to the structure.[11] It is attributed to the diagonal transition between the lower state of the injector miniband and the fundamental subband 1. We show in Fig. 3(b) the difference between the energy positions of the two Gaussian functions ($\Delta E = E_2 - E_R$), fitting the spectra at different values of the current. By increasing the current, ΔE achieves a minimum, which is the tunnel coupling constant between the states R and 2. The computed splittings are 2.6 meV for GaInAs, 2.4 meV for GaAs, and 1.7 meV for InAs. The agreement is quite good for GaAs and GaInAs; on the contrary, concerning InAs, the measured splitting is almost twice the calculated one. The full width at half maximum (FWHM) of the Gaussian functions is shown in Fig. 3(c). The larger width corresponds to the low energy Gaussian function, in agreement with the diagonal nature of this transition.[11] It decreases when increasing current until a minimum value. On the contrary, the width of the direct transition, which is half the diagonal one, is approximately constant with respect to the current. This is consistent with a weak coupling regime between the injector and state 2. It is worth noting that the spectra are well fitted by Gaussian functions only when the states R and 2 are in resonance. In this case, the wavefunctions of state 2 strongly delocalize into the injector. This has the double effect of making the transition $2 \rightarrow 1$ diagonal in the real space and producing an overlap with the impurities and interfaces of the injector, thus inducing the inhomogeneous broadening of the direct transition.[12,13] Far from this regime, the $2 \rightarrow 1$ transition has a Lorentzian shape. The values of the FWHM are very close for the three structures, indicating that the effects arising from the material quality are very similar.[14]

In conclusion, we have made a comparative study of the principal material systems for QCLs. We have shown that the QE (hence the gain) has the predicted dependence on $(m_e^*)^{-3/2}$. As a consequence InAs/AlSb is a very promising material system for QCL from the point of view of the gain, at least at 10 μm. Furthermore, we have shown that the shape of the electroluminescence spectra is very similar for the different material systems, indicating that it is strongly influenced by the design of the active region and by the tunneling mechanism. The comparison between the lineshapes indicates that the material quality of the three devices is very similar.

We gratefully acknowledge support from EU MRTN-CT-2004-51240 POISE.

[1] J. Faist, F. Capasso, D. L. Sivco, C. Sirtori, A. L. Hutchinson, and A. Y. Cho, Science **264**, 553 (1994).
[2] C. Sirtori, P. Kruck, S. Barbieri, P. Collot, J. Nagle, M. Beck, J. Faist, and U. Oesterle, Appl. Phys. Lett. **73**, 3486 (1998).
[3] K. Ohtani and H. Ohno, Appl. Phys. Lett. **82**, 1003 (2003).
[4] R. Teissier, D. Barate, A. Vicet, C. Alibert, A. N. Baranov, X. Marcadet, C. Renaud, M. Garcia, C. Sirtori, D. Revin, and J. Cockburn, Appl. Phys. Lett. **85**, 167 (2004).
[5] The GaInAs/AlInAs structure has been grown by MOVPE, while the GaAs/AlGaAs and InAs/AlSb structures have been obtained by MBE. The layer sequence in nanometers for one period of active region, starting from the injection barrier, is **5**/10.2/**4.6**/7/**2.6**/6.1/**2.4**/5.8/**2.4**/5.4/**2.4**/4.8/**2.8**/5/**2.4**/4.6 for GaInAs/AlInAs; **4.8**/8.6/**3.5**/5.5/**2.1**/4.7/**2.1**/4.2/**2.1**/3.9/**2.1**/3.8/**2.1**/3.7/**2.4**/3.6 for GaAs. Barriers are in bold; underlined layers are doped, 2×10^{17} cm^{-3} for the barriers and 4×10^{17} cm^{-3} for the wells. For InAs the layer sequence is **2.6**/14.8/**1.8**/11.7/**1.4**/9.8/**1**/9.5/**1**/8.5/**1**/8.1/**1**/7.6/**1.3**/7.3/**1.3**/7.3/**1**/7.3. Underlined layers are doped 5×10^{17} cm^{-3}.
[6] C. Sirtori, F. Capasso, J. Faist, and S. Scandolo, Phys. Rev. B **50**, 8663 (1994).
[7] The energy enters as $E_{21}{}^3$ in the spontaneous emission rate. The extra term comes from the photon energy.
[8] A. Leuliet, A. Vasanelli, A. Wade, G. Fedorov, D. Smirnov, G. Bastard, and C. Sirtori, Phys. Rev. B **73**, 085311 (2006).
[9] C. Faugeras, A. Wade, A. Leuliet, A. Vasanelli, C. Sirtori, G. Fedorov, D. Smirnov, R. Teissier, A. N. Baranov, D. Barate, and J. Devenson, Phys. Rev. B **74**, 113303 (2006).
[10] A. Vasanelli, A. Leuliet, C. Sirtori, A. Wade, G. Fedorov, D. Smirnov, G. Bastard, B. Vinter, M. Giovannini, and J. Faist, Appl. Phys. Lett. **89**, 172120 (2006).
[11] C. Sirtori, F. Capasso, J. Faist, A. L. Hutchinson, D. L. Sivco, and A. Y. Cho, IEEE J. Quantum Electron. **34**, 1722 (1998).
[12] S. Luin, V. Pellegrini, F. Beltram, X. Marcadet, and C. Sirtori, Phys. Rev. B **64**, 041306 (2001).
[13] K. L. Campman, H. Schmidt, A. Imamoglu, and A. C. Gossard, Appl. Phys. Lett. **69**, 2554 (1996).
[14] By assuming that the QW widths have a Gaussian distribution (which results in a Gaussian distribution of the energies), we found that the FWHM are compatible with a dispersion of the well widths of 1.4 Å for GaAs, 2.7 Å for GaInAs, and 2.8 Å for InAs.

This article is copyrighted as indicated in the article. Reuse of AIP content is subject to the terms at: http://scitation.aip.org/termsconditions. Downloaded to IP: 131.230.73.202 On: Thu, 18 Dec 2014 18:35:51